

# The Endothelial Prolyl-4-Hydroxylase Domain 2/Hypoxia-Inducible Factor 2 Axis Regulates Pulmonary Artery Pressure in Mice

Pinelopi P. Kapitsinou,<sup>a,b,c</sup> Ganeshkumar Rajendran,<sup>a,b</sup> Lindsay Astleford,<sup>a,b</sup> Mark Michael,<sup>c</sup> Michael P. Schonfeld,<sup>a,b</sup> Timothy Fields,<sup>b</sup> Sheila Shay,<sup>c</sup> Jaketa L. French,<sup>c</sup> James West,<sup>c</sup> Volker H. Haase<sup>c,d,e,f</sup>

Departments of Medicine, Anatomy, and Cell Biology<sup>a</sup> and The Kidney Institute,<sup>b</sup> University of Kansas Medical Center, Kansas City, Kansas, USA; Departments of Medicine,<sup>c</sup> Cancer Biology,<sup>d</sup> and Molecular Physiology and Biophysics,<sup>e</sup> Vanderbilt University School of Medicine, Nashville, Tennessee, USA; Medicine and Research Services, Department of Veterans Affairs Hospital, Tennessee Valley Healthcare System, Nashville, Tennessee, USA<sup>f</sup>

**Hypoxia-inducible factors 1 and 2 (HIF-1 and -2) control oxygen supply to tissues by regulating erythropoiesis, angiogenesis and vascular homeostasis. HIFs are regulated in response to oxygen availability by prolyl-4-hydroxylase domain (PHD) proteins, with PHD2 being the main oxygen sensor that controls HIF activity under normoxia. In this study, we used a genetic approach to investigate the endothelial PHD2/HIF axis in the regulation of vascular function. We found that inactivation of *Phd2* in endothelial cells specifically resulted in severe pulmonary hypertension (~118% increase in right ventricular systolic pressure) but not polycythemia and was associated with abnormal muscularization of peripheral pulmonary arteries and right ventricular hypertrophy. Concurrent inactivation of either *Hif1a* or *Hif2a* in endothelial cell-specific *Phd2* mutants demonstrated that the development of pulmonary hypertension was dependent on HIF-2 $\alpha$  but not HIF-1 $\alpha$ . Furthermore, endothelial HIF-2 $\alpha$  was required for the development of increased pulmonary artery pressures in a model of pulmonary hypertension induced by chronic hypoxia. We propose that these HIF-2-dependent effects are partially due to increased expression of vasoconstrictor molecule endothelin 1 and a concomitant decrease in vasodilatory apelin receptor signaling. Taken together, our data identify endothelial HIF-2 as a key transcription factor in the pathogenesis of pulmonary hypertension.**

Endothelial cells (ECs) provide barrier, transport, synthetic, and metabolic functions at the interface of blood and adjacent tissue, and they play a central role in the organism's response to hypoxia, as they regulate vascular tone, immune responses, hemostasis, and angiogenesis. Central mediators of hypoxia adaptation are hypoxia-inducible factors 1 and 2 (HIF-1 and HIF-2), pleiotropic heterodimeric basic helix-loop-helix transcription factors that regulate erythropoiesis, angiogenesis, vascular homeostasis, energy metabolism, and other oxygen-sensitive biological processes (1). HIF activity is controlled by O<sub>2</sub><sup>-</sup>, iron-, and ascorbate-dependent dioxygenases, also known as prolyl-4-hydroxylase domain-containing proteins 1 to 3 (PHD1 to PHD3), which use 2-oxoglutarate (2OG) as the substrate for the hydroxylation of specific proline residues within the oxygen-sensitive HIF- $\alpha$  subunit, PHD2 being the main oxygen sensor that regulates HIF activity under normoxia (2). The hydroxylation of HIF- $\alpha$  permits binding to the von Hippel-Lindau (VHL)-E3 ubiquitin ligase complex and results in proteasomal degradation of HIF- $\alpha$  subunits (3). When prolyl-4-hydroxylation is inhibited, e.g., in the absence of molecular oxygen or ferrous iron, HIF- $\alpha$  is no longer degraded and translocates to the nucleus, where it dimerizes with ARNT, the constitutively expressed HIF- $\beta$  subunit, and increases the transcription of oxygen-regulated genes (4).

In humans, genetic mutations in the PHD/HIF/VHL axis have been associated with multiple vascular pathologies. *VHL* germ line mutations result in a pleomorphic familial tumor syndrome, characterized by the development of highly vascularized tumors, which include central nervous system (CNS) and retinal hemangioblastomas, renal cell cancer, and pheochromocytomas (5). Furthermore, homozygosity for a hypomorphic *VHL* allele (R200W), which impairs the cell's ability to efficiently degrade HIF- $\alpha$  under normoxia, is associated with the development of polycythemia, pulmonary hypertension, and vertebral hemangi-

omas and increased incidence of cerebral vascular events (6, 7). Polycythemia and pulmonary hypertension have also been associated with rare activating mutations in the *HIF2A* locus (8). The critical role of HIF signaling in vascular development and pathogenesis is furthermore strongly supported by genetic studies with mice. For example, global inactivation of either *Hif1a* or *Arnt* resulted in embryonic lethality due to abnormal vascular development (9, 10), whereas *Hif2a* inactivation led to defects in embryonic vascular remodeling and other pathologies, which were genetic background dependent (11–14). Conversely, activation of HIF signaling via *Phd2* germ line ablation resulted in severe placental and heart defects that led to embryonic demise between embryonic days 12.5 and 14.5 (15), whereas global *Phd2* inactivation in adults led to excessive vascular growth and angiectasis in multiple organs (16). The promotion of vascular pathology as a result of PHD inactivation is a major clinical concern, as several HIF-activating PHD-inhibiting compounds are currently in phase 2 and 3 clinical trials for the treatment of renal anemia (17).

While genetic studies have found divergent functions for HIF-1 and HIF-2 in tumor angiogenesis, metastasis, maintenance

Received 6 December 2015 Returned for modification 22 December 2015

Accepted 9 March 2016

Accepted manuscript posted online 14 March 2016

Citation Kapitsinou PP, Rajendran G, Astleford L, Michael M, Schonfeld MP, Fields T, Shay S, French JL, West J, Haase VH. 2016. The endothelial prolyl-4-hydroxylase domain 2/hypoxia-inducible factor 2 axis regulates pulmonary artery pressure in mice. *Mol Cell Biol* 36:1584–1594. doi:10.1128/MCB.01055-15.

Address correspondence to Pinelopi P. Kapitsinou, pkapitsinou@kumc.edu.

Supplemental material for this article may be found at <http://dx.doi.org/10.1128/MCB.01055-15>.

Copyright © 2016, American Society for Microbiology. All Rights Reserved.

of lung endothelial barrier, and postischemic renal inflammation (18–23), relatively little is known about the role of endothelial PHDs in vascular homeostasis in the adult. To investigate the role of the endothelial PHD2/HIF axis in vascular homeostasis, we used a genetic approach and ablated *Phd2* individually or in conjunction with either *Hif1a* or *Hif2a* by Cre-loxP-mediated recombination. We found that loss of endothelial PHD2 induced pulmonary arterial hypertension and vascular remodeling in a HIF-2-dependent, and not HIF-1-dependent, fashion. We furthermore show that endothelial HIF-2 is required for the development of hypoxia-induced pulmonary hypertension and thus demonstrate that genetic manipulations of HIF-2 signaling in ECs specifically are sufficient to alter pulmonary vascular responses to hypoxia. Taken together, our findings identify endothelial HIF-2 as a potential therapeutic target for the treatment of pulmonary hypertension. Furthermore, our data have implications for the clinical use of PHD inhibitors as erythropoiesis-stimulating agents (ESA) in patients with advanced chronic kidney disease, who are predisposed to the development of pulmonary hypertension (24).

## MATERIALS AND METHODS

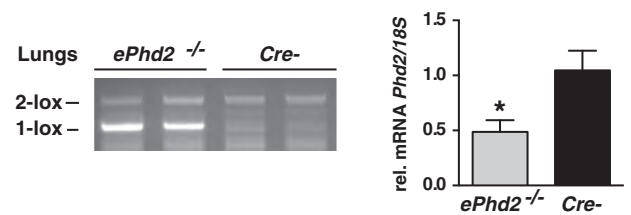
**Generation of mice, genotyping, and animal procedures.** The generation and genotyping of *Phd2*, *Hif1a*, and *Hif2a* (also known as *Epas1*) 2-lox alleles have been described previously (10, 25, 26). For the activation or inactivation of PHD2, HIF-1 $\alpha$ , and HIF-2 $\alpha$  in ECs, *VE-cadherin* (*Cdh5*)-cre transgenic mice were used (27).

Transthoracic echocardiography was conducted using a Vevo 770 high-resolution image system (VisualSonics, Toronto) (28). Right ventricular systolic pressure (RVSP) was measured invasively by inserting a 1.4F Mikro-tip catheter transducer (Millar Instruments, Houston, TX) into a surgically exposed right internal jugular vein, as described elsewhere (29). Systolic blood pressure (SBP) was measured in conscious mice at room temperature using a tail cuff monitor (BP-2000 BP analysis system; Visitech System). An animal hypoxia chamber from Biospherix, Ltd., was used for *in vivo* hypoxia experiments. Bone marrow transplantation was performed as previously described (20), and chimeric mice were subjected to hypoxia 5 weeks following transplantation. For pharmacological HIF activation, HIF prolyl-4-hydroxylase inhibitor GSK1002083A (Glaxo-SmithKline) was dissolved in 1% methylcellulose and administered by oral gavage at a dose of 60 mg/kg of body weight (BW). Complete blood counts were determined with a Hemavet 950 analyzer (Drew Scientific). Blood glucose levels were measured with the iSTAT portable clinical analyzer (Abbott portable handheld clinical analyzers). All procedures involving mice were performed in accordance with NIH guidelines for the use and care of live animals and were approved by the Institutional Animal Care and Use Committee (IACUC) of Vanderbilt University and the University of Kansas.

**DNA, RNA, and protein analyses.** DNA and RNA were isolated and used for genomic or real-time PCR analysis as previously described (20); mouse primer sequences used are shown in Table S1 in the supplemental material. For the detection of HIF-1 $\alpha$  and HIF-2 $\alpha$  by immunoblotting, nuclear protein extracts were prepared and analyzed as previously described (30).

**Morphological analysis.** For the morphological analysis, agarose-inflated lungs were fixed with 10% buffered formalin. Macrophage infiltration and cell proliferation were assessed with a monoclonal rat anti-F4/80 antibody and a polyclonal rabbit anti-Ki67 antiserum, respectively (Abcam, Inc.). To assess vessel muscularization of peripheral blood vessels, an anti- $\alpha$ -smooth muscle actin (anti- $\alpha$ SMA) antibody (Boster Bio) was used. For all morphological quantifications, 10 random visual fields were analyzed per lung section at a magnification of  $\times 200$  using ImageJ software (<http://rsbweb.nih.gov/ij>).

## A.



## B.

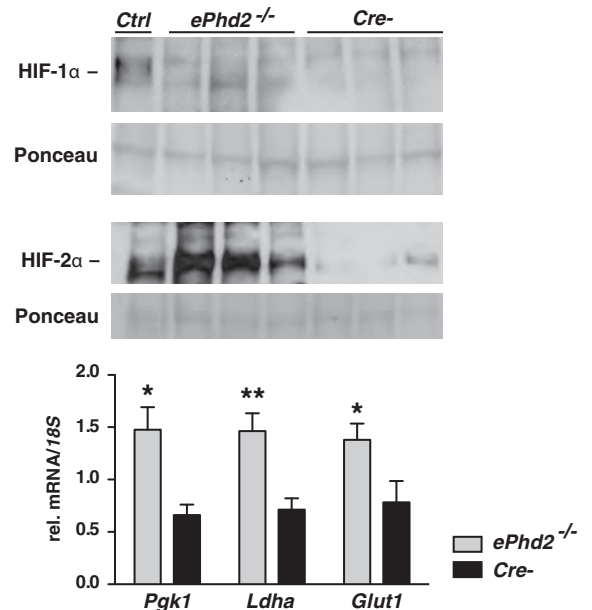


**FIG 1** EC-specific inactivation of *Phd2* stabilizes HIF-1 $\alpha$  and HIF-2 $\alpha$ . (A) (Left) Genomic PCR analysis of DNA isolated from the lungs of *ePhd2*<sup>-/-</sup> mutants and *Cre*<sup>-/-</sup> control mice. Primers used amplified both the conditional (2-lox) and the recombined (1-lox) alleles. (Right) *Phd2* transcript levels in whole lung homogenates from *ePhd2*<sup>-/-</sup> mutants and *Cre*<sup>-/-</sup> littermate controls ( $n = 7$ ;  $P = 0.02$ ). (B) (Top) Immunoblot analysis of HIF-1 $\alpha$  and HIF-2 $\alpha$  in lung nuclear extracts isolated from *ePhd2*<sup>-/-</sup> and *Cre*<sup>-/-</sup> mice. Ponceau S staining was used to assess for equal protein loading. Nuclear kidney extracts from a mouse treated with an oral PHD inhibitor served as a positive control (Ctrl). (Bottom) *Pdk1*, *Ldha*, and *Glut1* mRNA levels in lungs from mutant mice compared to those from *Cre*<sup>-/-</sup> littermate controls ( $n = 6$ ). Bars represent mean values  $\pm$  SEM. \*,  $P < 0.05$ ; \*\*,  $P < 0.01$ .

**Statistical analysis.** All data are reported as mean values  $\pm$  standard errors of the means (SEM). Statistical analyses were performed with Prism 5.0b (GraphPad Software, La Jolla, CA). Univariate analysis was done using the Student *t* test, and a two-sided significance level of 5% was considered statistically significant.

## RESULTS

**Generation of mice with EC-specific inactivation of *Phd2*.** To investigate the role of endothelial PHD2 in the pulmonary vasculature, we crossed *Cdh5*-cre transgenic mice (27) to mice homozygous for the conditional *Phd2* allele (26), hereafter designated *ePhd2*<sup>-/-</sup> mutants. *Cdh5*-cre is expressed in  $>90\%$  of pulmonary ECs, as previously shown by our laboratory (20), and genomic PCR analysis confirmed efficient excision of the floxed *Phd2* sequence (Fig. 1A). Accordingly, *Phd2* transcript levels showed a 2.1-fold reduction in total lung homogenates from *ePhd2*<sup>-/-</sup> mu-

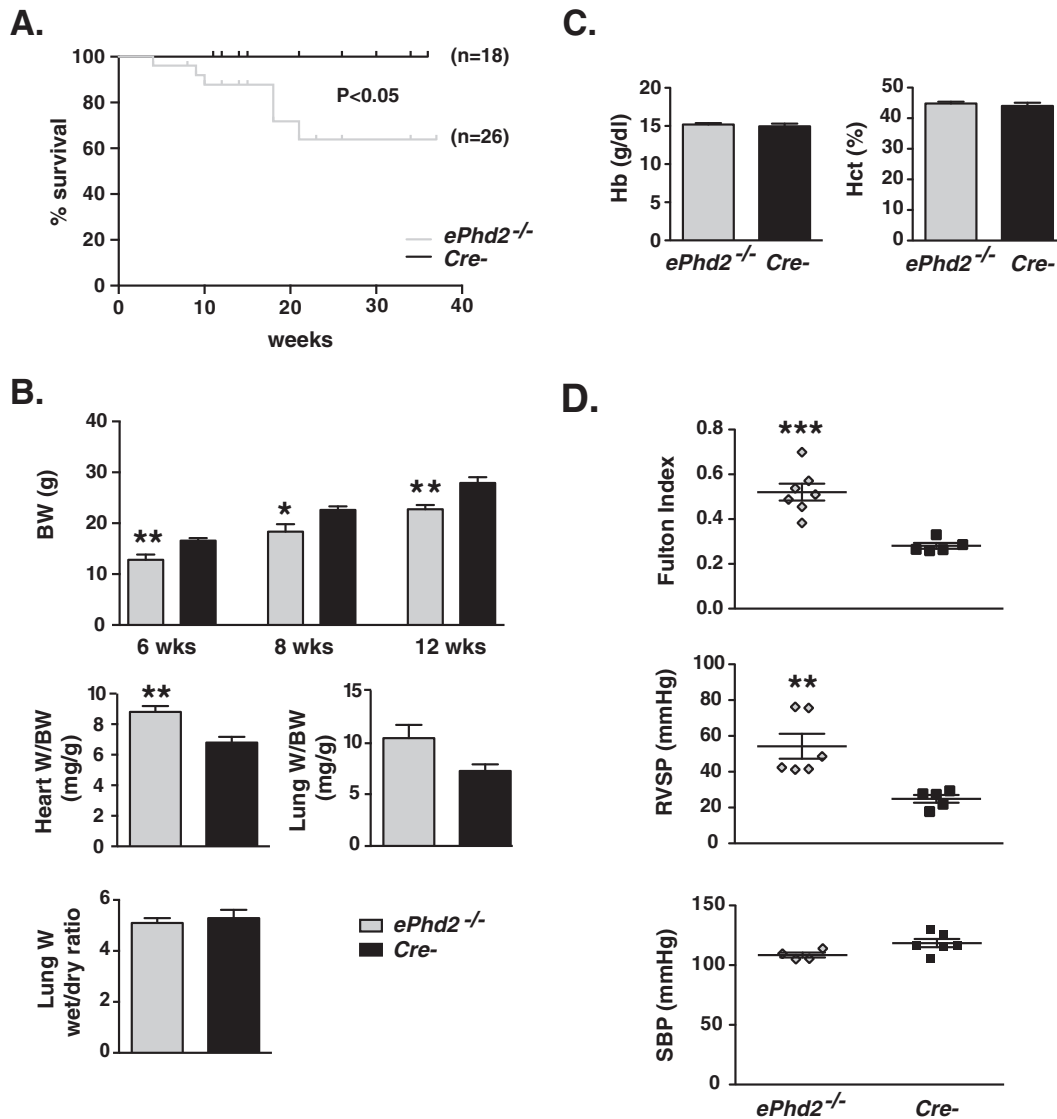


**FIG 2** Endothelial *Phd2* inactivation results in premature mortality and pulmonary hypertension associated with right ventricular hypertrophy. (A) Shown are Kaplan-Meier survival curves for mutants and control mice. (B) The top panel shows body weights (BW) for *ePhd2*<sup>-/-</sup> mice and *Cre*<sup>-</sup> controls at 6, 8, and 12 weeks of age ( $n = 5$  to  $10$ ). The middle panels depict ratios of heart or lung weight (W) to BW (heart,  $n = 8$  or  $9$ ; lung,  $n = 3$  or  $4$ ). The bottom panel shows the ratio of wet weight to dry weight for lungs from *ePhd2*<sup>-/-</sup> mutants and littermate controls ( $n = 5$  or  $6$ ). (C) Hemoglobin (Hb) concentration and hematocrit (Hct) levels in *ePhd2*<sup>-/-</sup> mutants and controls ( $n = 5$ ). Bars represent mean values  $\pm$  SEM. \*,  $P < 0.05$ ; \*\*,  $P < 0.01$ . (D) Fulton index [(RV/(LV+S))], right ventricular systolic pressure (RVSP) ( $n = 5$  or  $6$ ), and systolic blood pressure (SBP) in *ePhd2*<sup>-/-</sup> mice and *Cre*<sup>-</sup> controls ( $n = 4$  to  $6$ ). Bars represent mean values  $\pm$  SEM. \*,  $P < 0.05$ ; \*\*,  $P < 0.01$ ; \*\*\*,  $P < 0.001$ .

tants ( $n = 7$ ;  $P = 0.02$ ) (Fig. 1A). EC-specific inactivation of *Phd2* resulted in significant HIF-2 $\alpha$  accumulation in whole lung homogenates, whereas a change in HIF-1 $\alpha$  levels was not apparent (Fig. 1B). However, since glycolytic genes are predominantly regulated by HIF-1 and not HIF-2 (1), increased HIF-1 activity was suggested by the expression of *Pgk1* and *Ldha* being increased 2.2- and 2.1-fold, respectively ( $n = 4$ ) (Fig. 1B). *Glut1* was increased 1.8-fold (Fig. 1B).

**Inactivation of endothelial *Phd2* results in pulmonary hypertension.** While birth rates were not significantly different from the frequencies expected based on Mendelian genetics, *ePhd2*<sup>-/-</sup> mutants had a significantly shorter life span (Fig. 2A). By 6 weeks of age, total body weight (BW) was reduced by  $\sim 30\%$  ( $P = 0.007$ ;

$n = 5$  or  $6$ ) (Fig. 2B). While the PHD2/HIF axis is important in the regulation of erythropoiesis and glucose homeostasis (17, 31), EC-specific *Phd2* inactivation did not produce polycythemia or abnormalities in blood glucose levels (Fig. 2C; see also Fig. S1 in the supplemental material). In contrast to findings for the kidneys and spleen (see Fig. S1B), *ePhd2*<sup>-/-</sup> mutants displayed a 29% increase in heart weight/BW ratio ( $P = 0.0023$ ;  $n = 8$  or  $9$ ) and a 45% increase in lung weight/BW ratio, raising the possibility that *ePhd2*<sup>-/-</sup> mutants were predisposed to the development of congestive heart failure ( $P = 0.038$ ;  $n = 4$  to  $6$ ) (Fig. 2B). However, comparison of wet to dry lung weights was not consistent with elevated pulmonary water content (Fig. 2B).

Given the increase in heart weights, we next performed cardiac

TABLE 1 Echocardiographic parameters for *ePhd2*<sup>-/-</sup> and *Cre*<sup>-</sup> mice<sup>a</sup>

Parameter	Value for:	
	<i>ePhd2</i> <sup>-/-</sup> mice (n = 7)	<i>Cre</i> <sup>-</sup> mice (n = 5)
Heart rate (beats/min)	387 ± 10	383 ± 20
LVIDd (mm)	3.79 ± 0.28	3.12 ± 0.27
LVIDs (mm)	2.18 ± 0.29	1.66 ± 0.25
Fractional shortening (%)	42 ± 5	46 ± 5
PA area (mm <sup>2</sup> )	3.58 ± 0.27	2.49 ± 0.13**
PAAT (ms)	13.9 ± 2.1	22.0 ± 1.2*
RV stroke vol (mm <sup>3</sup> )	64 ± 6	46 ± 4*

<sup>a</sup>Data are means ± SEM. LVIDd, left ventricular internal diameter at diastole; LVIDs, left ventricular internal diameter at systole; PA, pulmonary artery; PAAT, pulmonary artery acceleration time; RV, right ventricular. \*, *P* < 0.05; \*\*, *P* < 0.01.

sonography in 10- to 12-week-old mice. Although we did not find significant changes in heart rate and parameters of left ventricular (LV) function (normal fractional shortening), *ePhd2*<sup>-/-</sup> mutant mice displayed significant increases in pulmonary artery (PA) area (3.58 ± 0.27 mm<sup>2</sup> versus 2.49 ± 0.13 mm<sup>2</sup> in controls; *n* = 5 to 7; *P* = 0.0098) and right ventricular (RV) stroke volume (64 ± 6 mm<sup>3</sup> versus 46 ± 4 mm<sup>3</sup> in controls; *n* = 5 to 7; *P* = 0.04), which were associated with a reduction in PA acceleration time (PAAT) (13.93 ± 2.10 ms versus 22 ± 1.22 ms in controls; *n* = 5 to 7; *P* = 0.01) (Table 1). Furthermore, deletion of endothelial *Phd2* resulted in right ventricular hypertrophy (RVH), which was assessed by the Fulton index, calculated as the weight ratio between RV and LV plus septum; *ePhd2*<sup>-/-</sup> mice exhibited an 86% increase in the Fulton index compared to that of the controls (*P* = 0.0004; *n* = 5 to 7) (Fig. 2D). Taken together, anatomic and echocardiographic findings were consistent with RV remodeling, which is likely to be secondary to pulmonary hypertension. To assess PA pressures directly, we next performed right heart catheterization via right jugular vein access and found increased RVSP (54.23 ± 6.93 mm Hg versus 24.84 ± 2.17 mm Hg in controls; *P* = 0.005, *n* = 5 or 6), confirming the presence of pulmonary hypertension in *ePhd2*<sup>-/-</sup> mutants (Fig. 2D). A difference in SBP between the mutants and controls was not found (Fig. 2D).

Despite RVH and the significant increase in RVSP, morphological analysis of *ePhd2*<sup>-/-</sup> lungs by hematoxylin and eosin (H&E) staining did not demonstrate plexiform or lumen-obliterating lesions, both hallmarks of severe pulmonary hypertension in humans (32) (Fig. 3A). However, enhanced muscularization of peripheral pulmonary arteries was detected in mutants compared to controls, as indicated by an increase in the number of arteries with diameters of <100 μm that stained positive for αSMA (22.1 ± 1.6 versus 7.6 ± 1.5 muscularized vessels/10 high-power fields [HPF]; *n* = 5 to 7; *P* < 0.0001) (Fig. 3B). Remarkably, we observed patchy areas of alveolar injury, which exhibited increased αSMA expression and F4/80<sup>+</sup> cell infiltration in ~60% of *ePhd2*<sup>-/-</sup> mice (see Fig. S2 in the supplemental material). However, most of the lung parenchyma had normal morphology, and quantification of F4/80<sup>+</sup> cells in random optical fields showed no significant difference between mutants and controls (Fig. 3B). We next examined the expression of proliferation marker Ki67. In *ePhd2*<sup>-/-</sup> mutants, we found an ~32% reduction in the number of Ki67<sup>+</sup> cells in areas of normal lung parenchyma compared to that in controls (*P* = 0.03; *n* = 5 to 7) (Fig. 3B), whereas areas of alveolar injury displayed a significant increase in Ki67<sup>+</sup> cells (see Fig. S2). In summary, our data demonstrate that inactivation of

*Phd2* in ECs alone is sufficient to induce pulmonary hypertension, pulmonary vascular remodeling, and RVH in mice. Since *Cdh5*-*Cre* activity is not limited to pulmonary endothelium alone and targets all vascular beds, we cannot completely exclude that *Phd2* deletion in cardiac ECs by itself has contributed to the development of RVH independently of the elevated pulmonary artery pressures.

**Inactivation of HIF-2 but not HIF-1 reverses pulmonary hypertension in *ePhd2*<sup>-/-</sup> mice.** To dissect the contribution of individual HIF homologs to the development of pulmonary hypertension in *ePhd2*<sup>-/-</sup> mice, we used the *Cdh5-cre* transgene to generate mice that were concomitantly deficient for either *Phd2* and *Hif-1α* or *Phd2* and *Hif-2α*, hereafter referred to as either *ePhd2*<sup>-/-</sup> *Hif1a*<sup>-/-</sup> or *ePhd2*<sup>-/-</sup> *Hif2a*<sup>-/-</sup> mutants. As predicted, concurrent inactivation of *Phd2* and *Hif-1α* in ECs resulted in a significant accumulation of HIF-2α, whereas differences in HIF-1α levels were not detected between lungs from mutant and control mice (Fig. 4A). Efficient inactivation of HIF-1 signaling was reflected in the normalization of *Pgk1*, *Ldha*, *Pdk1*, and *Pdk3* mRNA levels in lungs from *ePhd2*<sup>-/-</sup> *Hif1a*<sup>-/-</sup> mice compared to those from *ePhd2*<sup>-/-</sup> mice (Fig. 4A; see also Fig. S3 in the supplemental material). Although an increase in HIF-1α protein levels was difficult to demonstrate in lungs from *ePhd2*<sup>-/-</sup> *Hif2a*<sup>-/-</sup> mice, increased HIF-1 activity in lungs from *ePhd2*<sup>-/-</sup> *Hif2a*<sup>-/-</sup> mice was suggested by a 2.7-fold increase of *Pgk1* transcript levels compared to those in controls (*P* = 0.0012; *n* = 6) (Fig. 4A) as well as significant induction in the expression of other glycolytic genes (see Fig. S3). In contrast to the findings for *ePhd2*<sup>-/-</sup> *Hif1a*<sup>-/-</sup> mutants, HIF-2α levels were no longer elevated (Fig. 4A).

To determine to what degree individual *Phd2/Hif* double mutants developed pulmonary hypertension, we performed detailed morphological studies and right heart catheterizations. We found that RVSP was significantly increased in *ePhd2*<sup>-/-</sup> *Hif1a*<sup>-/-</sup> mutants (40.83 ± 2.44 mm Hg versus 23.40 ± 0.54 mm Hg in controls; *n* = 3 or 4; *P* = 0.0005), which was associated with the development of significant RVH as indicated by a 2.5-fold increase in the Fulton index (*P* = 0.0004; *n* = 4 to 6) (Fig. 4B). In contrast to findings for the *ePhd2*<sup>-/-</sup> *Hif1a*<sup>-/-</sup> mutants, inactivation of *Hif2a* reversed RVH and pulmonary hypertension, restoring RVSP and the Fulton index to control levels (Fig. 4B). In keeping with the results from the hemodynamic measurements, small-vessel muscularization was increased in lungs from *ePhd2*<sup>-/-</sup> *Hif1a*<sup>-/-</sup> mice but not in those from *ePhd2*<sup>-/-</sup> *Hif2a*<sup>-/-</sup> mice (25.5 ± 3.8 muscularized vessels/10 HPF in *ePhd2*<sup>-/-</sup> *Hif1a*<sup>-/-</sup> mutants versus 8.2 ± 1.2 muscularized vessels/10 HPF in controls; *n* = 4 or 5; *P* = 0.0057) (Fig. 4C). Taken together, these findings demonstrate that the activation of HIF-2 but not HIF-1 signaling is responsible for the development of pulmonary hypertension and its associated its associated morphological changes in mice with endothelial *Phd2* inactivation.

**Endothelial HIF-2 is required for the development of hypoxia-induced pulmonary hypertension.** Our genetic analysis demonstrated that endothelial HIF-2 was required for the development of pulmonary hypertension in mice with *Phd2* inactivation. We next wished to investigate its role in a non-*Phd2*-deficient genetic background. For this, we chose a model of pulmonary hypertension induced by hypoxia, a common clinical trigger of increased PA pressure. For this purpose, 8-week-old mice that lacked HIF-2α in ECs (C57BL/6 background), hereafter referred

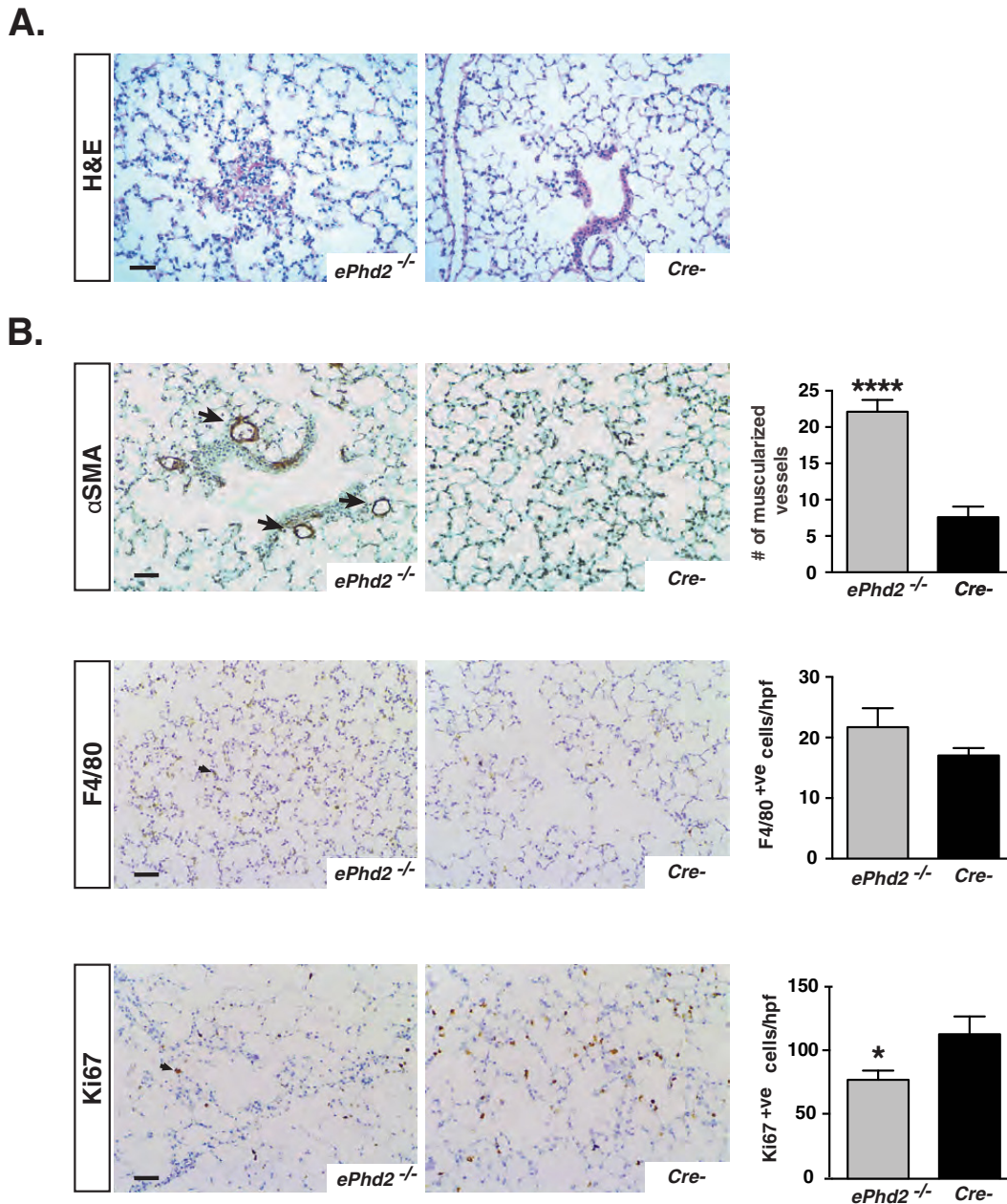


**FIG 3** Histopathological characterization of mice lacking endothelial *Phd2*. (A) Representative images of H&E-stained lungs from *ePhd2*<sup>-/-</sup> mutants and *Cre*<sup>-</sup> control mice at 10 weeks of age. (B) Representative images of  $\alpha$ SMA-, F4/80-, and Ki67-stained lungs from *ePhd2*<sup>-/-</sup> mice and littermate controls. Arrows identify  $\alpha$ SMA<sup>+</sup>ve arterioles (top), F4/80<sup>+</sup>ve cells (middle), and Ki67<sup>+</sup>ve cells (bottom). Graphs show quantification of muscularized vessel number/10 HPF, F4/80<sup>+</sup> cell number/HPF, and Ki67<sup>+</sup> cell number/HPF ( $n = 5$  to  $7$ ). Graph bars represent mean values  $\pm$  SEM. \*,  $P < 0.05$ ; \*\*\*\*,  $P < 0.0001$ . Scale bars indicate 50  $\mu$ m.

to as *eHif2a*<sup>-/-</sup> mice, and their *Cre*<sup>-</sup> littermate controls were exposed to 10% O<sub>2</sub> in a normobaric hypoxia chamber. After exposure to hypoxia for 4 weeks, mice of the two genotypes developed comparable degrees of erythrocytosis (hematocrits [Hcts] of 62%  $\pm$  2% in *eHif2a*<sup>-/-</sup> mice versus 61%  $\pm$  1% in *Cre*<sup>-</sup> mice;  $n = 4$  to  $6$ ). Remarkably, *eHif2a*<sup>-/-</sup> mutants did not display any evidence of hypoxia-induced pulmonary hypertension or RVH, while *Cre*<sup>-</sup> control mice developed the predicted increase in RVSP (20.78  $\pm$  0.64 mm Hg in *eHif2a*<sup>-/-</sup> mutants versus 28.82  $\pm$  0.69 mm Hg in controls;  $n = 4$  to  $6$ ;  $P < 0.0001$ ) and Fulton index

(increase by 50%;  $P = 0.0003$ ) (Fig. 5A). Furthermore, hypoxia provoked pulmonary vascular remodeling only in *Cre*<sup>-</sup> control mice, which contained significantly higher numbers of muscularized vessels than did *eHif2a*<sup>-/-</sup> mutants (9.6  $\pm$  1.7 in *eHif2a*<sup>-/-</sup> mice versus 17.7  $\pm$  1.5 muscularized vessels/10 HPF in controls;  $n = 4$  to  $6$ ;  $P = 0.009$ ) (Fig. 5B). Collectively, these data provide evidence that endothelial HIF-2 signaling is required for the development of hypoxia-induced pulmonary hypertension in mice that are wild type (WT) for PHD2.

Since *VE-cadherin* promoter-driven Cre recombinase is ex-

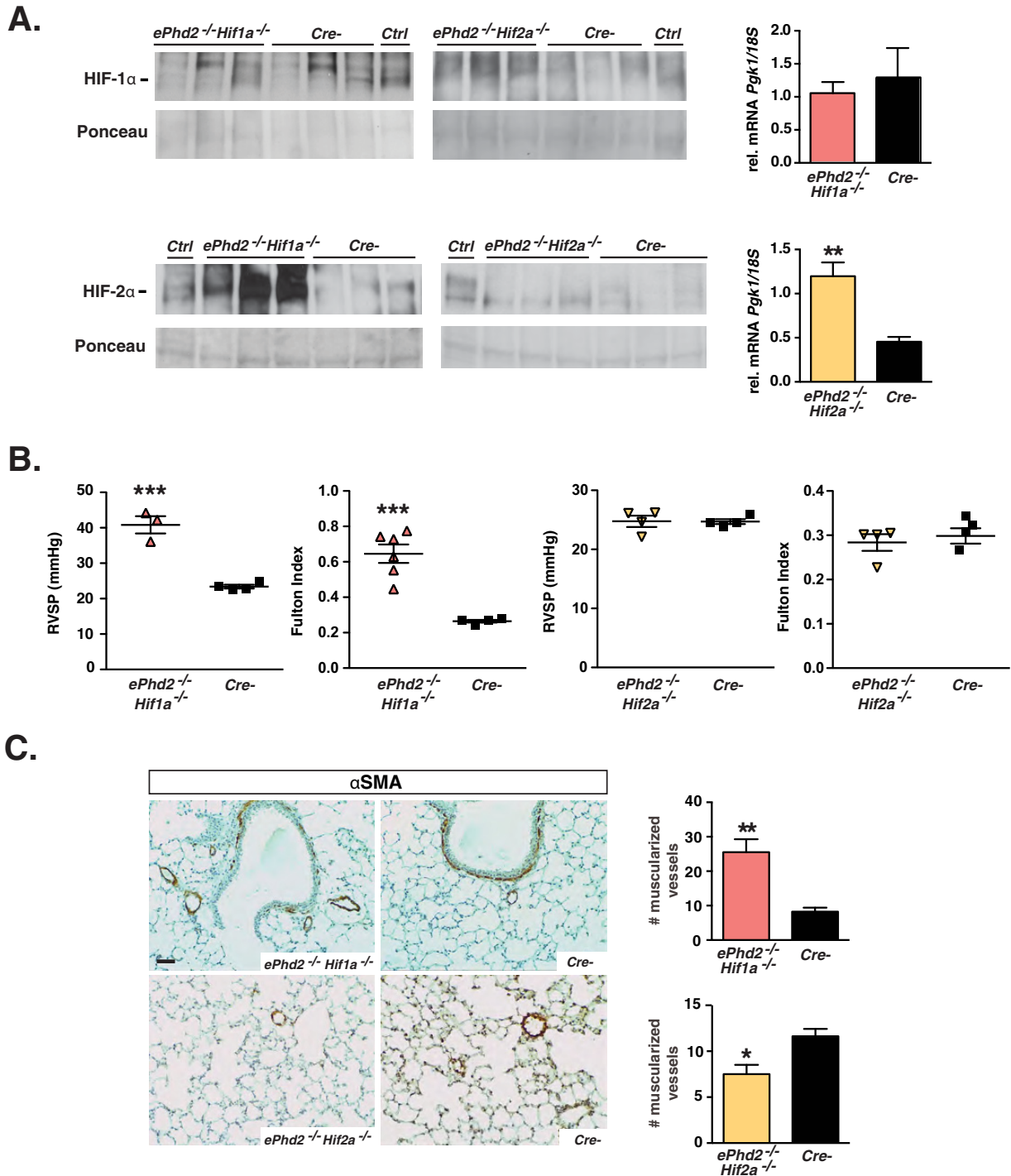


**FIG 4** Pulmonary hypertension in *ePhd2*<sup>-/-</sup> mice is dependent on HIF-2. (A) Shown are HIF-1α (top) and HIF-2α (bottom) protein levels as detected by immunoblot analysis of nuclear pulmonary extracts from *ePhd2*<sup>-/-</sup> *Hif1a*<sup>-/-</sup> mice, *ePhd2*<sup>-/-</sup> *Hif2a*<sup>-/-</sup> mice, and their *Cre*<sup>-</sup> littermate controls. Nuclear protein extracts from the kidney or liver of a PHI-treated mouse were used as positive controls (Ctrl). Ponceau staining was used to assess for equal protein loading. The graphs depict *Pgk1* transcript levels in lungs from *ePhd2*<sup>-/-</sup> *Hif1a*<sup>-/-</sup> (*n* = 6) and *ePhd2*<sup>-/-</sup> *Hif2a*<sup>-/-</sup> (*n* = 5) mice. (B) RVSP and Fulton index in *ePhd2*<sup>-/-</sup> *Hif1a*<sup>-/-</sup> and *ePhd2*<sup>-/-</sup> *Hif2a*<sup>-/-</sup> mice. (C) Representative images of lungs stained for αSMA and quantification of muscularized vessels expressed as number/10 HPF in *ePhd2*<sup>-/-</sup> *Hif1a*<sup>-/-</sup>, *ePhd2*<sup>-/-</sup> *Hif2a*<sup>-/-</sup>, and control mice. Bars represent mean values ± SEM. \*, *P* < 0.05; \*\*, *P* < 0.01; \*\*\*, *P* < 0.001. Scale bar, 50 μm.

pressed in hematopoietic cells (27), we carried out bone marrow transplantation experiments to exclude the possibility that *Hif2a* inactivation in hematopoietic cells was contributory. We found that transplantation of *eHif2a*<sup>-/-</sup> bone marrow cells into lethally

irradiated WT mice did not prevent the hypoxia-induced increases in RVSP and the Fulton index compared to those in WT mice transplanted with WT bone marrow (Fig. 5C). These data suggest that *Cdh5*-*Cre*-mediated inactivation of *Hif2a* in hemato-

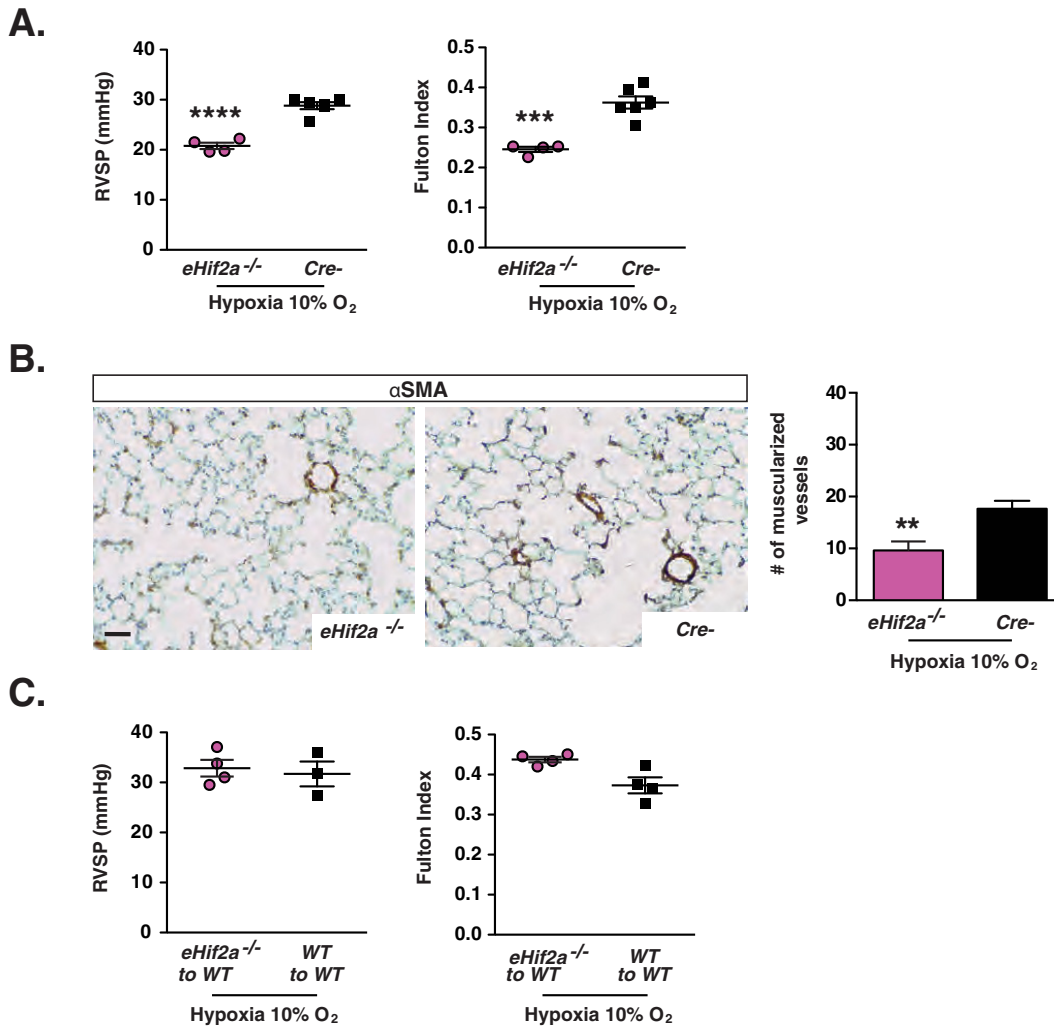


**FIG 5** Inactivation of endothelial *Hif2a* protects from the development of hypoxia-induced pulmonary hypertension. (A) Shown are RVSP and Fulton index measurements performed for *eHif2a*<sup>-/-</sup> and *Cre*<sup>-</sup> mice following chronic normobaric hypoxia (10% O<sub>2</sub> for 4 weeks) ( $n = 4$  to  $6$ ). (B) Representative images of lungs stained for  $\alpha$ SMA, with the graph depicting muscularized vessel number/10 HPF in *eHif2a*<sup>-/-</sup> and *Cre*<sup>-</sup> mice following chronic hypoxic exposure (10% O<sub>2</sub> for 4 weeks) ( $n = 4$  to  $6$ ). (C) RVSP ( $n = 3$  or  $4$ ) and Fulton index ( $n = 4$ ) in transplanted WT mice subjected to chronic normobaric hypoxia (10% O<sub>2</sub> for 4 weeks). *eHif2a*<sup>-/-</sup> to WT, WT mice transplanted with bone marrow cells from *eHif2a*<sup>-/-</sup> mutants; WT to WT, WT mice transplanted with bone marrow cells from WT mice. Bars represent mean values  $\pm$  SEM. \*\*,  $P < 0.01$ ; \*\*\*,  $P < 0.001$ ; \*\*\*\*,  $P < 0.0001$ . Scale bar, 50  $\mu$ m.

poietic cells is not sufficient to protect from pulmonary hypertension and furthermore support the notion that endothelial HIF-2 alone is required for the development of pulmonary hypertension induced by chronic hypoxia.

**Differential roles for HIF-1 and HIF-2 in the regulation of endothelin 1 and apelin receptor signaling.** Because hypoxia regulates endothelin 1 (EDN1) (33, 34), a potent vasoconstrictor, but also apelin (APLN) (35, 36), a vasodilatory peptide acting through binding to the apelin G-protein-coupled receptor (APLNR), we next assessed the role of the endothelial HIF-2 axis in the regulation of these molecules. Endothelial deletion of *Phd2* resulted in a 6.4-fold induction of pulmonary *Edn1* mRNA ( $P = 0.029$ ;  $n = 8$ ) but not *Apln* mRNA (Fig. 6). In contrast, *Aplnr* was downregulated 2.5-fold in *ePhd2*<sup>-/-</sup> mutants ( $P = 0.037$ ;  $n = 8$ ) (Fig. 6). A similar pattern of expression was detected in *ePhd2*<sup>-/-</sup> *Hif1a*<sup>-/-</sup> mice (Fig. 6), whereas simultaneous deletion of *Hif2a* and *Phd2* reversed these changes. Specifically, *ePhd2*<sup>-/-</sup> *Hif2a*<sup>-/-</sup> mutants

exhibited a 2.3-fold reduction in *Edn1* mRNA ( $n = 6$ ;  $P = 0.03$ ), a 2.8-fold increase in *Apln* transcripts ( $n = 6$ ;  $P = 0.0002$ ), and no change in *Aplnr* transcript levels (Fig. 6). Similar changes, although not statistically significant, were noted in *eHif2a*<sup>-/-</sup> mice subjected to chronic hypoxia (Fig. 6). *Cre*<sup>-</sup> control mice subjected to chronic hypoxia displayed only minor changes in gene expression compared to that in normoxic controls, which is most likely due to physiologic adaptation to prolonged hypoxia, e.g., erythrocytosis.

To investigate the differences between acute and chronic hypoxia, we next examined the effects of acute HIF activation on *Edn1* and *Apln/Aplnr* gene expression *in vivo*. To model acute hypoxia, we subjected WT mice to 8% O<sub>2</sub> for 48 h and maintained control littermates in room air. Acute hypoxia resulted in 4.3-fold and 1.6-fold upregulation of *Edn1* and *Apln* transcripts, respectively ( $P = 0.0011$  for *Edn1*;  $P = 0.08$  for *Apln*;  $n = 4$  or  $5$ ), while *Aplnr* was reduced 4.3-fold ( $P = 0.0005$ ;  $n = 4$  or  $5$ ) (Fig. 7). We ob-

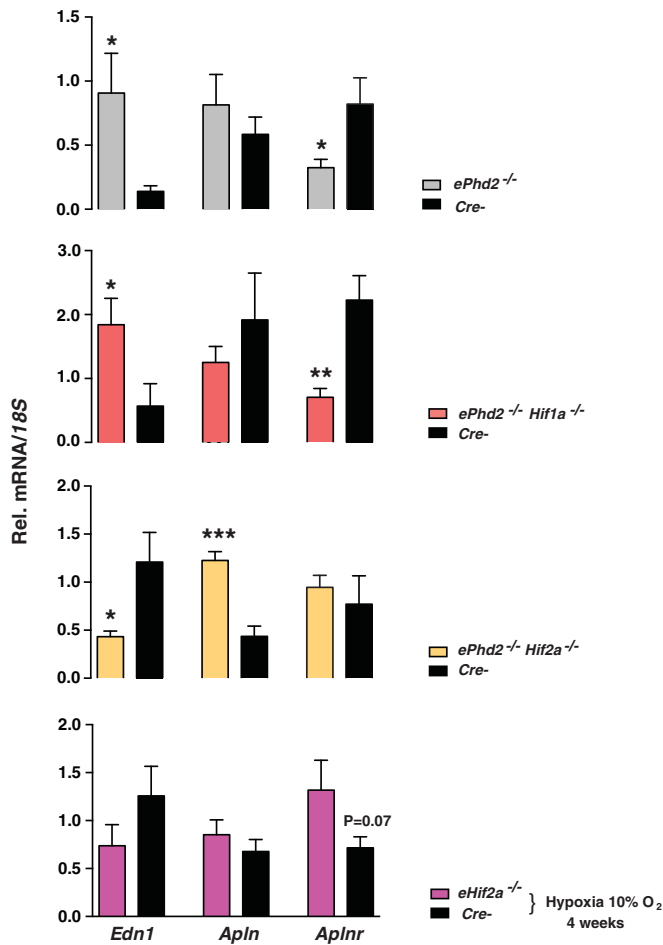


**FIG 6** HIF-2 regulates pulmonary *Edn1* and *Aplnr* expression. Relative levels of *Edn1*, *Apln*, and *Aplnr* mRNAs in *ePhd2*<sup>-/-</sup> (*n* = 8), *ePhd2*<sup>-/-</sup> *Hif1a*<sup>-/-</sup> (*n* = 5), *ePhd2*<sup>-/-</sup> *Hif2a*<sup>-/-</sup> (*n* = 6), and *eHif2a*<sup>-/-</sup> (*n* = 4 to 6) mice following chronic normobaric hypoxia (10% O<sub>2</sub> for 4 weeks) and in their corresponding *Cre*<sup>-</sup> littermate controls. 18S was used for normalization. Bars represent mean values ± SEM. \*, *P* < 0.05; \*\*, *P* < 0.01; \*\*\*, *P* < 0.001.

served similar gene expression changes in mice treated with a prolyl-4-hydroxylase inhibitor (PHI) that results in global HIF activation (30) (Fig. 7). Specifically, treatment with PHI upregulated *Edn1* and *Apln* transcripts 6.6- and 2.6-fold, respectively (*P* < 0.0001 for *Edn1*; *P* = 0.02 for *Apln*; *n* = 4 or 5), while a 3.3-fold reduction was noted for *Aplnr* (*P* = 0.002; *n* = 4 or 5).

While EDN1 and APLN have previously been shown to be HIF regulated in ECs, the suppression of *Aplnr* in hypoxia conflicted with prior studies proposing that APLNR was induced in hypoxic murine lungs, human stellate cells, and hepatocytes (37, 38). Because in lungs, both ECs and smooth muscle cells express APLNR, we next examined whether the effects of endothelial HIF-2 activation on *Aplnr* gene expression *in vivo* were (i) reproducible and (ii) direct in cultured ECs. To address these questions, we conducted hypoxia experiments (0.5% O<sub>2</sub> for 24 h) with human umbilical cord vein endothelial cells (HUVEC) in the presence or absence of *HIF2a* or *ARNT* using a small interfering RNA (siRNA) approach. Although hypoxia resulted in significant downregulation of APLNR mRNA, this response appeared to be HIF independent. In contrast to APLNR, the hypoxic induction of APLN was blunted in

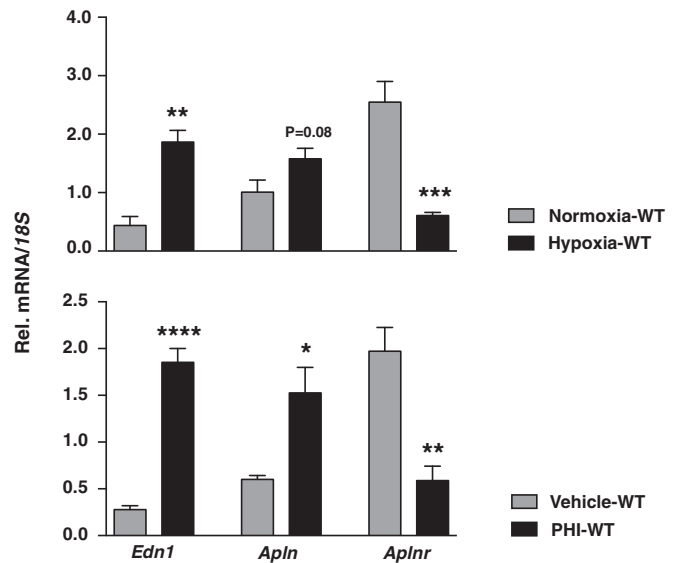


**FIG 7** Hypoxia and pharmacological PHD inhibition induce *Edn1* and suppress *Aplnr*. (Top) Relative levels of *Edn1*, *Apln* and *Aplnr* in mice subjected to acute normobaric hypoxia (8% O<sub>2</sub> for 2 days) compared to normoxic controls (*n* = 4 or 5). (Bottom) *Edn1*, *Apln*, and *Aplnr* transcript levels in mice treated with prolyl-4-hydroxylase inhibitor GSK1002083A compared to vehicle-treated controls (*n* = 4 or 5). 18S was used for normalization. Bars represent mean values ± SEM. \*, *P* < 0.05; \*\*, *P* < 0.01; \*\*\*, *P* < 0.001; \*\*\*\*, *P* < 0.0001.

HUVEC treated with siRNA against *HIF2a* (see Fig. S4 in the supplemental material). The discrepancy between these findings and our *in vivo* data may have resulted from species-related differences or differences in hypoxic signaling between different EC subtypes (vein EC versus arterial EC), or it could be a reflection of context-specific hypoxic gene regulation. Nevertheless, our *in vivo* data provide strong genetic evidence that activation of endothelial HIF-2 specifically promotes pulmonary vasoconstriction, which associates with dysregulation of EDN1 and APLNR signaling.

## DISCUSSION

In the present study, we used a genetic approach to dissect the role of the endothelial PHD2/HIF axis in the regulation of vascular homeostasis. Utilizing different conditional knockout strains, in which *Phd2* was inactivated in conjunction with either *Hif1a* or *Hif2a*, we obtained experimental evidence that endothelial PHD2 regulates PA pressure through HIF-2 but not HIF-1. We furthermore identified endothelial HIF-2 as a central mediator in the development of hypoxia-induced pulmonary hypertension that is independent of hypoxia-associated polycythemia, and we propose that HIF-2 promotes pulmonary hypertension, at least partially, through the increased expression of vasoconstrictor molecule EDN1 and a concomitant decrease in vasodilatory APLNR signaling.

Pulmonary hypertension resulting from systemic hypoxia or global HIF-2 activation is frequently associated with polycythemia, as kidneys respond to chronic hypoxia or HIF-2 activation with increased erythropoietin (EPO) production (17), raising the possibility that polycythemia by itself is an important pathogenic factor in the development of hypoxia/HIF-2-induced pulmonary hypertension. For example, elevations in resting PA pressures with heightened hypoxia responses have been documented



for humans with inherited erythrocytosis due to HIF-2 gain-of-function mutations or nontumorigenic VHL mutations (Chuvash polycythemia) (7, 39–41). Mice homozygous for the VHL-Chuvash mutation (R200W) spontaneously developed pulmonary hypertension and RVH in a HIF-2-dependent manner (42), a phenotype that was also recapitulated in transgenic mice that carried a HIF-2 $\alpha$  gain-of-function mutation (G536W) (43). Since EPO-producing cells are not targeted in *ePhd2*<sup>-/-</sup> mice, we were able to dissociate the effects of HIF-2 activation on PA pressure from its effects on erythropoiesis. Our data clearly demonstrate that polycythemia was not required for the development of HIF-2-induced pulmonary hypertension. The fact that HIF-2-induced erythrocytosis does not always associate with pulmonary hypertension, e.g., in humans and mice heterozygous for certain *Phd2* mutations (39, 41), is likely due to tissue-specific differences in the regulation of HIF-2 $\alpha$  stability or sensitivity to small increases in HIF-2 transcriptional activity.

While our data establish that HIF-2 $\alpha$  is the critical HIF- $\alpha$  homolog regulating pulmonary vascular responses, increased HIF-1 $\alpha$  expression has been observed in PA-derived medial smooth muscle cells and within human plexiform lesions, a morphological hallmark of idiopathic pulmonary arterial hypertension (IPAH), suggesting that HIF1-dependent signaling may contribute to IPAH-associated proliferative vasculopathy (44). In mice, global heterozygous *Hif1a* deficiency dampened pulmonary vascular responses induced by prolonged hypoxia, a finding that suggested a role for HIF-1 in the pathogenesis of hypoxia-induced pulmonary hypertension. However, studies aimed at dissecting the contribution of HIF-1 in a cell-type-specific manner generated conflicting results. Inducible deletion of *Hif1a* in smooth muscle cells using a smooth muscle myosin heavy chain (*SMMHC*)-*CreER*<sup>T2</sup> transgenic line significantly attenuated hypoxia-induced pulmonary hypertension and the associated remodeling of pulmonary arteries (45), whereas inactivation of *Hif1a* achieved by use of a constitutive smooth muscle protein 22  $\alpha$  (*SM22a*)-*Cre* transgenic line increased pulmonary vascular tone under both normoxic and hypoxic conditions without inducing vascular remodeling (46). Because ECs from lungs of patients with IPAH showed evidence of HIF-1 activation and because of HIF-1's involvement in the regulation of energy metabolism, it has been suggested that endothelial HIF-1 may have disease-promoting effects by switching cellular metabolism from oxidative phosphorylation to glycolysis (47), a process that has been shown to be important for tumor growth. Remarkably, our study found that HIF-1 does not regulate PA pressure in *ePhd2*<sup>-/-</sup> mutant mice. Furthermore, although endothelial HIF-1 activity was significantly increased in *ePhd2*<sup>-/-</sup>*Hif2*<sup>-/-</sup> mutants and was associated with the induction of glycolytic genes, PA pressures were completely normal and pulmonary hypertension did not develop. Consistent with these findings is that the loss of endothelial HIF-2 $\alpha$  alone was sufficient to confer complete protection from hypoxia-induced pulmonary hypertension. Interestingly, an independent study reported that endothelial HIF-2 deficiency promoted the development of pulmonary hypertension in aged mice. While this report suggested that HIF-2 was protecting from pulmonary hypertension, it is plausible that the development of pulmonary hypertension in aged *eHif2a*<sup>-/-</sup> animals was secondary to loss of lung endothelial barrier function, which was reported in this model (22).

Our genetic studies identified ECs as a key cell type in the pathogenesis of hypoxia-induced pulmonary hypertension. Consistent with our findings is a crucial role for ECs in the pathogenesis of IPAH, as shown by studies in which EC-specific deletion of

bone morphogenic protein receptor type II (*Bmpr2*) was sufficient for the induction of pulmonary hypertension in a subset of mice (48). Conversely, restoration of endothelial BMPR-II expression reversed experimentally induced pulmonary hypertension (49). Notably, we found that the reversal of pulmonary hypertension in *ePhd2*<sup>-/-</sup>*Hif2a*<sup>-/-</sup> mice was associated with induction of *Bmpr2*, while treatment with PHI suppressed *Bmpr2*, suggesting a potential role for HIF-2 in the regulation of BMPR-II levels (see Fig. S5A in the supplemental material). The molecular mechanisms by which loss of BMPR-II in ECs promotes pulmonary hypertension remain ill-defined but may involve a paradoxical increase in EC apoptosis followed by excessive clonal proliferation (32). Furthermore, a recent study showed that *miR-130/301*, a key regulator of EC proliferation in both hereditary and acquired forms of pulmonary hypertension, operates under the control of HIF-2 (50). However, we did not find significant alterations in the expression of *miR-130a* and *miR-301a* in *ePhd2*<sup>-/-</sup> or PHI-treated mice (see Fig. S5B). Nevertheless, mice with EC-specific *Phd2* inactivation did not show a significant hyperproliferative response or obstructive cellular lesions, raising the possibility that certain EC-mediated responses in the context of hypoxia-induced pulmonary hypertension are distinct from those in IPAH.

Hypoxia, among other triggers, promotes sustained vasoconstriction and vascular remodeling by modulating the production of growth factors and vasoactive mediators in ECs (51). For example, EDN1, a small peptide released from ECs, induces potent vasoconstriction upon binding to its receptors on smooth muscle cells. In agreement with the previously established role of EDN1 in hypoxia-induced pulmonary hypertension (52), we found that increased pulmonary *Edn1* mRNA levels were associated with the presence of pulmonary hypertension in our genetic models. Although prior studies have shown that *Edn1* is coregulated by HIF-1 and HIF-2 (33, 42), we demonstrate that endothelial PHD2 controls the expression of *Edn1* via HIF-2. In contrast to the case with EDN1, the HIF-2-dependent suppression of *Aplnr* was an unexpected finding and suggested that abnormal vasodilatory APLN signaling may have contributed to hypoxia-induced pulmonary hypertension. Given that HIF-2 usually acts as a transcriptional activator and not suppressor (53), HIF-2-dependent suppression of *Aplnr* transcription is likely to have occurred indirectly. Prior studies with rat cardiomyocytes and adipocytes have shown that the APLNR ligand APLN is HIF-1 inducible (35, 36). This is in agreement with the increased expression of *Apln* in *ePhd2*<sup>-/-</sup>*Hif2*<sup>-/-</sup> mice. However, *Apln* expression was significantly blunted in *ePhd2*<sup>-/-</sup> mutants, which suggested that HIF-2 is likely to suppress APLN synthesis despite the presence of HIF-1 $\alpha$ . Taken together, our findings support a concept where the endothelial PHD2/HIF-2 axis blunts APLN-mediated vasodilatory effects by inhibiting *Aplnr* expression and by limiting HIF-1-dependent induction of *Apln*. Consistent with this model are previous studies in which APLN-mediated effects on vascular tone were lost under hypoxic conditions (54). Furthermore, two genetic APLNR variants (rs11544374 and rs2282623) were associated with a predisposition to high-altitude pulmonary edema, reinforcing the concept that APLNR signaling plays a critical role in hypoxia-induced vascular responses in the lungs (55).

In summary, we have shown by a genetic approach that activation of HIF-2 signaling in ECs plays a critical role in the pathogenesis of pulmonary hypertension. Our findings justify careful cardiovascular evaluations of patients that participate in clinical trials

of HIF-2-activating PHD inhibitors for the treatment of renal anemia (17). However, pharmacological inhibition of HIF-2 signaling (56, 57) may represent a novel approach for treating pulmonary hypertension.

## ACKNOWLEDGMENTS

We thank William G. Kaelin for providing *Phd2<sup>fl/fl</sup>* mice, Bing Yao and Ming-Zhi Zhang for technical assistance with the bone marrow transplantation experiments, and Kevin J. Duffy (GlaxoSmithKline) for providing the HIF prolyl-4-hydroxylase inhibitor GSK1002083A.

This work was supported by an American Heart Association National Scientist Development grant (11SDG5570023 to P.P.K.), the Carl Gottschalk Award of the American Society of Nephrology (P.P.K.), and National Institutes of Health (NIH) grants P20 GM104936 (P.P.K.) and R01-HL095797 (J.W.). V.H.H. was supported by the Krick-Brooks Chair in Nephrology, NIH grants R01-DK081646, R01-DK080821, and R01-DK101791, and a Department of Veterans Affairs merit award (1101BX002348).

The funders had no role in study design, data collection and interpretation, or the decision to submit the work for publication.

P.P.K. and V.H.H. conceived the experiments; P.P.K., G.R., L.A., M.M., M.P.S., S.S., and J.L.F. performed experiments; P.P.K., G.R., L.A., M.M., M.P.S., T.F., S.S., J.W., and V.H.H. analyzed and interpreted data; and P.P.K. and V.H.H. wrote the manuscript.

Volker H. Haase serves on the Scientific Advisory Board of Akebia Therapeutics, a company that develops prolyl-4-hydroxylase inhibitors for the treatment of anemia.

## FUNDING INFORMATION

This work, including the efforts of Pinelopi P. Kapitsinou, was funded by HHS | National Institutes of Health (NIH) (P20 GM104936). This work, including the efforts of James West, was funded by HHS | National Institutes of Health (NIH) (R01-HL095797). This work, including the efforts of Volker H Haase, was funded by HHS | National Institutes of Health (NIH) (R01-DK081646, R01-DK080821, and R01-DK101791). This work, including the efforts of Volker H Haase, was funded by U.S. Department of Veterans Affairs (VA) (1101BX002348). This work, including the efforts of Pinelopi P. Kapitsinou, was funded by American Heart Association (AHA) (11SDG5570023). This work, including the efforts of Pinelopi P. Kapitsinou, was funded by American Society of Nephrology (ASN).

## REFERENCES

- Majmundar AJ, Wong WJ, Simon MC. 2010. Hypoxia-inducible factors and the response to hypoxic stress. *Mol Cell* 40:294–309. <http://dx.doi.org/10.1016/j.molcel.2010.09.022>.
- Loenarz C, Schofield CJ. 2008. Expanding chemical biology of 2-oxoglutarate oxygenases. *Nat Chem Biol* 4:152–156. <http://dx.doi.org/10.1038/nchembio0308-152>.
- Kaelin WG, Jr, Ratcliffe PJ. 2008. Oxygen sensing by metazoans: the central role of the HIF hydroxylase pathway. *Mol Cell* 30:393–402. <http://dx.doi.org/10.1016/j.molcel.2008.04.009>.
- Wenger RH, Stiehl DP, Camenisch G. 2005. Integration of oxygen signaling at the consensus HRE. *Sci STKE* 2005:re12.
- Maher ER, Kaelin WG, Jr. 1997. von Hippel-Lindau disease. *Medicine (Baltimore)* 76:381–391. <http://dx.doi.org/10.1097/00005792-199711000-00001>.
- Gordeuk VR, Sergueeva AI, Miasnikova GY, Okhotin D, Voloshin Y, Choyke PL, Butman JA, Jedlickova K, Prchal JT, Polyakova LA. 2004. Congenital disorder of oxygen sensing: association of the homozygous Chuvash polycythemia VHL mutation with thrombosis and vascular abnormalities but not tumors. *Blood* 103:3924–3932. <http://dx.doi.org/10.1182/blood-2003-07-2535>.
- Smith TG, Brooks JT, Balanos GM, Lappin TR, Layton DM, Leedham DL, Liu C, Maxwell PH, McMullin MF, McNamara CJ, Percy MJ, Pugh CW, Ratcliffe PJ, Talbot NP, Treacy M, Robbins PA. 2006. Mutation of von Hippel-Lindau tumour suppressor and human cardiopulmonary physiology. *PLoS Med* 3:e290. <http://dx.doi.org/10.1371/journal.pmed.0030290>.
- Gale DP, Harten SK, Reid CDL, Tuddenham EGD, Maxwell PH. 2008. Autosomal dominant erythrocytosis and pulmonary arterial hypertension associated with an activating HIF2 mutation. *Blood* 112:919–921. <http://dx.doi.org/10.1182/blood-2008-04-153718>.
- Maltepe E, Schmidt JV, Baunoch D, Bradfield CA, Simon MC. 1997. Abnormal angiogenesis and responses to glucose and oxygen deprivation in mice lacking the protein ARNT. *Nature* 386:403–407. <http://dx.doi.org/10.1038/386403a0>.
- Ryan HE, Lo J, Johnson RS. 1998. HIF-1 alpha is required for solid tumor formation and embryonic vascularization. *EMBO J* 17:3005–3015. <http://dx.doi.org/10.1093/emboj/17.11.3005>.
- Compernelle V, Brusselmans K, Acker T, Hoet P, Tjwa M, Beck H, Plaisance S, Dor Y, Keshet E, Lupu F, Nemery B, Dewerchin M, Van Veldhoven P, Plate K, Moons L, Collen D, Carmeliet P. 2002. Loss of HIF-2alpha and inhibition of VEGF impair fetal lung maturation, whereas treatment with VEGF prevents fatal respiratory distress in premature mice. *Nat Med* 8:702–710.
- Peng J, Zhang L, Drysdale L, Fong GH. 2000. The transcription factor EPAS-1/hypoxia-inducible factor 2alpha plays an important role in vascular remodeling. *Proc Natl Acad Sci U S A* 97:8386–8391. <http://dx.doi.org/10.1073/pnas.140087397>.
- Scortegagna M, Ding K, Oktay Y, Gaur A, Thurmond F, Yan LJ, Marck BT, Matsumoto AM, Shelton JM, Richardson JA, Bennett MJ, Garcia JA. 2003. Multiple organ pathology, metabolic abnormalities and impaired homeostasis of reactive oxygen species in *Epas1*<sup>-/-</sup> mice. *Nat Genet* 35:331–340. <http://dx.doi.org/10.1038/ng1266>.
- Tian H, Hammer RE, Matsumoto AM, Russell DW, McKnight SL. 1998. The hypoxia-responsive transcription factor EPAS1 is essential for catecholamine homeostasis and protection against heart failure during embryonic development. *Genes Dev* 12:3320–3324. <http://dx.doi.org/10.1101/gad.12.21.3320>.
- Takeda K, Ho V, Takeda H, Duan L, Nagy A, Fong G. 2006. Placental but not heart defects are associated with elevated hypoxia-inducible factor alpha levels in mice lacking prolyl hydroxylase domain protein 2. *Mol Cell Biol* 26:8336–8346. <http://dx.doi.org/10.1128/MCB.00425-06>.
- Takeda K, Cowan A, Fong GH. 2007. Essential role for prolyl hydroxylase domain protein 2 in oxygen homeostasis of the adult vascular system. *Circulation* 116:774–781. <http://dx.doi.org/10.1161/CIRCULATIONAHA.107.701516>.
- Koury MJ, Haase VH. 2015. Anaemia in kidney disease: harnessing hypoxia responses for therapy. *Nat Rev Nephrol* 11:394–410. <http://dx.doi.org/10.1038/nrneph.2015.82>.
- Branco-Price C, Zhang N, Schnelle M, Evans C, Katschinski DM, Liao D, Ellies L, Johnson RS. 2012. Endothelial cell HIF-1α and HIF-2α differentially regulate metastatic success. *Cancer Cell* 21:52–65. <http://dx.doi.org/10.1016/j.ccr.2011.11.017>.
- Gong H, Rehman J, Tang H, Wary K, Mittal M, Chatturvedi P, Zhao Y, Komorova YA, Vogel SM, Malik AB. 2015. HIF2α signaling inhibits adherens junctional disruption in acute lung injury. *J Clin Invest* 125:652–664. <http://dx.doi.org/10.1172/JCI77701>.
- Kapitsinou PP, Sano H, Michael M, Kobayashi H, Davidoff O, Bian A, Yao B, Zhang M-Z, Harris RC, Duffy KJ, Erickson-Miller CL, Sutton TA, Haase VH. 2014. Endothelial HIF-2 mediates protection and recovery from ischemic kidney injury. *J Clin Invest* 124:2396–2409. <http://dx.doi.org/10.1172/JCI69073>.
- Manalo DJ, Rowan A, Lavoie T, Natarajan L, Kelly BD, Ye SQ, Garcia JG, Semenza GL. 2005. Transcriptional regulation of vascular endothelial cell responses to hypoxia by HIF-1. *Blood* 105:659–669. <http://dx.doi.org/10.1182/blood-2004-07-2958>.
- Skuli N, Liu L, Runge A, Wang T, Yuan L, Patel S, Iruela-Arispe L, Simon MC, Keith B. 2009. Endothelial deletion of hypoxia-inducible factor-2alpha (HIF-2alpha) alters vascular function and tumor angiogenesis. *Blood* 114:469–477. <http://dx.doi.org/10.1182/blood-2008-12-193581>.
- Tang N, Wang L, Esko J, Giordano FJ, Huang Y, Gerber HP, Ferrara N, Johnson RS. 2004. Loss of HIF-1alpha in endothelial cells disrupts a hypoxia-driven VEGF autocrine loop necessary for tumorigenesis. *Cancer Cell* 6:485–495. <http://dx.doi.org/10.1016/j.ccr.2004.09.026>.
- Sise ME, Courtwright AM, Channick RN. 2013. Pulmonary hypertension in patients with chronic and end-stage kidney disease. *Kidney Int* 84:682–692. <http://dx.doi.org/10.1038/ki.2013.186>.

25. Gruber M, Hu CJ, Johnson RS, Brown EJ, Keith B, Simon MC. 2007. Acute postnatal ablation of Hif-2alpha results in anemia. *Proc Natl Acad Sci U S A* 104:2301–2306. <http://dx.doi.org/10.1073/pnas.0608382104>.
26. Minamishima YA, Moslehi J, Bardeesy N, Cullen D, Bronson RT, Kaelin WG, Jr. 2008. Somatic inactivation of the PHD2 prolyl hydroxylase causes polycythemia and congestive heart failure. *Blood* 111:3236–3244. <http://dx.doi.org/10.1182/blood-2007-10-117812>.
27. Alva JA, Zovein AC, Monvoisin A, Murphy T, Salazar A, Harvey NL, Carmeliet P, Iruela-Arispe ML. 2006. VE-cadherin-Cre-recombinase transgenic mouse: a tool for lineage analysis and gene deletion in endothelial cells. *Dev Dyn* 235:759–767. <http://dx.doi.org/10.1002/dvdy.20643>.
28. West J, Niswender KD, Johnson JA, Pugh ME, Gleaves L, Fessel JP, Hemmes AR. 2013. A potential role for insulin resistance in experimental pulmonary hypertension. *Eur Respir J* 41:861–871. <http://dx.doi.org/10.1183/09031936.00030312>.
29. West J, Harral J, Lane K, Deng Y, Ickes B, Crona D, Albu S, Stewart D, Fagan K. 2008. Mice expressing BMPR2R899X transgene in smooth muscle develop pulmonary vascular lesions. *Am J Physiol Lung Cell Mol Physiol* 295:L744–L755. <http://dx.doi.org/10.1152/ajplung.90255.2008>.
30. Kapitsinou PP, Liu Q, Unger TL, Rha J, Davidoff O, Keith B, Epstein JA, Moores SL, Erickson-Miller CL, Haase VH. 2010. Hepatic HIF-2 regulates erythropoietic responses to hypoxia in renal anemia. *Blood* 116:3039–3048. <http://dx.doi.org/10.1182/blood-2010-02-270322>.
31. Ichiki T, Sunagawa K. 2014. Novel roles of hypoxia response system in glucose metabolism and obesity. *Trends Cardiovasc Med* 24:197–201. <http://dx.doi.org/10.1016/j.tcm.2014.03.004>.
32. Rabinovitch M. 2012. Molecular pathogenesis of pulmonary arterial hypertension. *J Clin Invest* 122:4306–4313. <http://dx.doi.org/10.1172/JCI60658>.
33. Camenisch G, Stroka DM, Gassmann M, Wenger RH. 2001. Attenuation of HIF-1 DNA-binding activity limits hypoxia-inducible endothelin-1 expression. *Pflügers Arch* 443:240–249. <http://dx.doi.org/10.1007/s004240100679>.
34. Minchenko A, Caro J. 2000. Regulation of endothelin-1 gene expression in human microvascular endothelial cells by hypoxia and cobalt: role of hypoxia responsive element. *Mol Cell Biochem* 208:53–62. <http://dx.doi.org/10.1023/A:1007042729486>.
35. Glassford AJ, Yue P, Sheikh AY, Chun HJ, Zarafshar S, Chan DA, Reaven GM, Quertermous T, Tsao PS. 2007. HIF-1 regulates hypoxia- and insulin-induced expression of apelin in adipocytes. *Am J Physiol Endocrinol Metab* 293:E1590–E1596. <http://dx.doi.org/10.1152/ajpendo.00490.2007>.
36. Ronkainen V-P, Ronkainen JJ, Hänninen SL, Leskinen H, Ruas JL, Pereira T, Poellinger L, Vuolteenaho O, Tavi P. 2007. Hypoxia inducible factor regulates the cardiac expression and secretion of apelin. *FASEB J* 21:1821–1830. <http://dx.doi.org/10.1096/fj.06-7294com>.
37. Chandra SM, Razavi H, Kim J, Agrawal R, Kundu RK, de Jesus Perez V, Zamanian RT, Quertermous T, Chun HJ. 2011. Disruption of the apelin-APJ system worsens hypoxia-induced pulmonary hypertension. *Arterioscler Thromb Vasc Biol* 31:814–820. <http://dx.doi.org/10.1161/ATVBAHA.110.219980>.
38. Melgar-Lesmes P, Pauta M, Reichenbach V, Casals G, Ros J, Bataller R, Morales-Ruiz M, Jiménez W. 2011. Hypoxia and proinflammatory factors upregulate apelin receptor expression in human stellate cells and hepatocytes. *Gut* 60:1404–1411. <http://dx.doi.org/10.1136/gut.2010.234690>.
39. Bigham AW, Lee FS. 2014. Human high-altitude adaptation: forward genetics meets the HIF pathway. *Genes Dev* 28:2189–2204. <http://dx.doi.org/10.1101/gad.250167.114>.
40. Formenti F, Beer PA, Croft QPP, Dorrington KL, Gale DP, Lappin TRJ, Lucas GS, Maher ER, Maxwell PH, McMullin MF, O'Connor DF, Percy MJ, Pugh CW, Ratcliffe PJ, Smith TG, Talbot NP, Robbins PA. 2011. Cardiopulmonary function in two human disorders of the hypoxia-inducible factor (HIF) pathway: von Hippel-Lindau disease and HIF-2alpha gain-of-function mutation. *FASEB J* 25:2001–2011. <http://dx.doi.org/10.1096/fj.10-177378>.
41. Lee FS, Percy MJ. 2011. The HIF pathway and erythrocytosis. *Annu Rev Pathol* 6:165–192. <http://dx.doi.org/10.1146/annurev-pathol-011110-130321>.
42. Hickey MM, Richardson T, Wang T, Mosqueira M, Arguiri E, Yu H, Yu Q-C, Solomides CC, Morrisey EE, Khurana TS. 2010. The von Hippel-Lindau Chuvash mutation promotes pulmonary hypertension and fibrosis in mice. *J Clin Invest* 120:827–839. <http://dx.doi.org/10.1172/JCI36362>.
43. Tan Q, Kerestes H, Percy MJ, Pietrofesa R, Chen L, Khurana TS, Christofidou-Solomidou M, Lappin TRJ, Lee FS. 2013. Erythrocytosis and pulmonary hypertension in a mouse model of human HIF2A gain of function mutation. *J Biol Chem* 288:17134–17144. <http://dx.doi.org/10.1074/jbc.M112.444059>.
44. Tuder RM, Chacon M, Alger L, Wang J, Taraseviciene-Stewart L, Kasahara Y, Cool CD, Bishop AE, Geraci M, Semenza GL, Yacoub M, Polak JM, Voelkel NF. 2001. Expression of angiogenesis-related molecules in plexiform lesions in severe pulmonary hypertension: evidence for a process of disordered angiogenesis. *J Pathol* 195:367–374. <http://dx.doi.org/10.1002/path.953>.
45. Ball MK, Waypa GB, Mungai PT, Nielsen JM, Czech L, Dudley VJ, Beussink L, Dettman RW, Berkelhamer SK, Steinhorn RH, Shah SJ, Schumacker PT. 2014. Regulation of hypoxia-induced pulmonary hypertension by vascular smooth muscle hypoxia-inducible factor-1α. *Am J Respir Crit Care Med* 189:314–324. <http://dx.doi.org/10.1164/rccm.201302-0302OC>.
46. Kim Y-M, Barnes EA, Alvira CM, Ying L, Reddy S, Cornfield DN. 2013. Hypoxia-inducible factor-1α in pulmonary artery smooth muscle cells lowers vascular tone by decreasing myosin light chain phosphorylation. *Circ Res* 112:1230–1233. <http://dx.doi.org/10.1161/CIRCRESAHA.112.300646>.
47. Fijalkowska I, Xu W, Comhair SAA, Janocha AJ, Mavrikis LA, Krishnamacharya B, Zhen L, Mao T, Richter A, Erzurum SC, Tuder RM. 2010. Hypoxia inducible-factor1alpha regulates the metabolic shift of pulmonary hypertensive endothelial cells. *Am J Pathol* 176:1130–1138. <http://dx.doi.org/10.2353/ajpath.2010.090832>.
48. Hong KH, Lee YJ, Lee E, Park SO, Han C, Beppu H, Li E, Raizada MK, Bloch KD, Oh SP. 2008. Genetic ablation of the Bmpr2 gene in pulmonary endothelium is sufficient to predispose to pulmonary arterial hypertension. *Circulation* 118:722–730. <http://dx.doi.org/10.1161/CIRCULATIONAHA.107.736801>.
49. Reynolds AM, Holmes MD, Danilov SM, Reynolds PN. 2012. Targeted gene delivery of BMPR2 attenuates pulmonary hypertension. *Eur Respir J* 39:329–343. <http://dx.doi.org/10.1183/09031936.00187310>.
50. Bertero T, Lu Y, Annis S, Hale A, Bhat B, Saggari R, Wallace WD, Ross DJ, Vargas SO, Graham BB, Kumar R, Black SM, Fratz S, Fineman JR, West JD, Haley KJ, Waxman AB, Chau BN, Cottrill KA, Chan SY. 2014. Systems-level regulation of microRNA networks by miR-130/301 promotes pulmonary hypertension. *J Clin Invest* 124:3514–3528. <http://dx.doi.org/10.1172/JCI74773>.
51. Shimoda LA, Laurie SS. 2014. HIF and pulmonary vascular responses to hypoxia. *J Appl Physiol* 116:867–874. <http://dx.doi.org/10.1152/jappphysiol.00643.2013>.
52. Galié N, Manes A, Branzi A. 2004. The endothelin system in pulmonary arterial hypertension. *Cardiovasc Res* 61:227–237. <http://dx.doi.org/10.1016/j.cardiores.2003.11.026>.
53. Schödel J, Oikonomopoulos S, Ragoussis J, Pugh CW, Ratcliffe PJ, Mole DR. 2011. High-resolution genome-wide mapping of HIF-binding sites by ChIP-seq. *Blood* 117:e207–e217. <http://dx.doi.org/10.1182/blood-2010-10-314427>.
54. Andersen CU, Markvardsen LH, Hilberg O, Simonsen U. 2009. Pulmonary apelin levels and effects in rats with hypoxic pulmonary hypertension. *Respir Med* 103:1663–1671. <http://dx.doi.org/10.1016/j.rmed.2009.05.011>.
55. Mishra A, Kohli S, Dua S, Thinlas T, Mohammad G, Pasha MAQ. 2015. Genetic differences and aberrant methylation in the apelin system predict the risk of high-altitude pulmonary edema. *Proc Natl Acad Sci U S A* 112:6134–6139. <http://dx.doi.org/10.1073/pnas.1422759112>.
56. Metelo AM, Noonan HR, Li X, Jin Y, Baker R, Kametsky L, Zhang Y, van Rooijen E, Shin J, Carpenter AE, Yeh J-R, Peterson RT, Iliopoulos O. 2015. Pharmacological HIF2α inhibition improves VHL disease-associated phenotypes in zebrafish model. *J Clin Invest* 125:1987–1997. <http://dx.doi.org/10.1172/JCI73665>.
57. Scheuermann TH, Li Q, Ma H-W, Key J, Zhang L, Chen R, Garcia JA, Naidoo J, Longgood J, Frantz DE, Tambar UK, Gardner KH, Bruick RK. 2013. Allosteric inhibition of hypoxia inducible factor-2 with small molecules. *Nat Chem Biol* 9:271–276. <http://dx.doi.org/10.1038/nchembio.1185>.